基于两性羧酸配体的Cu(Ⅱ)、Zn(Ⅱ)、Co(Ⅱ)、Mn(Ⅱ)配合物的合成、晶体结构及其与DNA相互作用

陈铭臻[1] 陈金香[2] 王若伦[1] 卢钧雄[1] 许雪飞*,[1]

([1]广州医科大学附属第二医院药学部,广州 510260)

([2]南方医科大学药学院,国家药品监督管理局药物代谢研究与评价重点实验室,广东省新药筛选重点实验室,广州 510515)

摘要: 以两性羧酸配体溴化*N*-(4-羧基苄基)异喹啉((HCbiq)Br)合成了4个新的金属配合物:$[Cu_2(Cbiq)_4(H_2O)_2]Br_4\cdot 2H_2O$ (**1**)、$[Zn(Cbiq)_2(H_2O)_2]Br_2\cdot Cbiq\cdot H_2O$ (**2**)、$[M_3(Cbiq)_8(\mu\text{-}OH)_2(H_2O)_2](ClO_4)_4\cdot 7H_2O$ (M=Co (**3**)、Mn (**4**))。通过单晶X射线衍射、元素分析和红外光谱表征了配合物**1**~**4**的结构。配合物**1**含有一个由4个Cbiq的羧基桥联双核Cu(Ⅱ)的结构,2个Cu(Ⅱ)还分别与一分子水配位。配合物**2**中,1个Zn(Ⅱ)分别与2个Cbiq的羧基氧原子进行单齿配位,同时还与2个水分子的氧原子进行配位。配合物**3**和**4**结构相似,均为三核结构。每2个M(Ⅱ)除了通过2个Cbiq的羧基上的氧进行桥联,还通过一个羟基的氧进行桥联。此外,2个端基的M(Ⅱ)分别与2个Cbiq的羧基进行单齿配位,同时还与一个水分子进行配位。凝胶电泳研究表明,配合物**1**可能是通过氧化机制在生理条件下有效切割DNA,其最大催化速率常数k_{max}为2.80 h^{-1},米氏常数K_M为3.22 $mmol\cdot L^{-1}$。溴化乙锭(EB)竞争实验表明配合物**1**具有较强的DNA结合亲和力。采用分子对接模拟计算得到配合物**1**与DNA的结合自由能为−49.87 $kJ\cdot mol^{-1}$。

关键词: 两性羧酸配体; 过渡金属配合物; 晶体结构; DNA

中图分类号: O614.121; O614.24+1; O614.81+2; O614.71+1 **文献标识码:** A **文章编号:** 1001-4861(2022)12-2499-12

DOI: 10.11862/CJIC.2022.241

Synthesis, Crystal Structures and DNA Interaction of Cu(Ⅱ), Zn(Ⅱ), Co(Ⅱ), and Mn(Ⅱ) Complexes Derived from Zwitterionic Carboxylate Ligand

CHEN Ming-Zhen[1] CHEN Jin-Xiang[2] WANG Ruo-Lun[1] LU Jun-Xiong[1] XU Xue-Fei*,[1]

([1]*Department of Pharmacy, The Second Affiliated Hospital of Guangzhou Medical University, Guangzhou* 510260, *China*)

([2]*NMPA Key Laboratory for Research and Evaluation of Drug Metabolism, Guangdong Provincial Key Laboratory of New Drug Screening, School of Pharmaceutical Sciences, Southern Medical University, Guangzhou* 510515, *China*)

Abstract: Four new metal complexes, namely $[Cu_2(Cbiq)_4(H_2O)_2]Br_4\cdot 2H_2O$ (**1**), $[Zn(Cbiq)_2(H_2O)_2]Br_2\cdot Cbiq\cdot H_2O$ (**2**), and $[M_3(Cbiq)_8(\mu\text{-}OH)_2(H_2O)_2](ClO_4)_4\cdot 7H_2O$ (M=Co (**3**), Mn (**4**)), were synthesized from the zwitterionic carboxylate ligand *N*-(4-carboxybenzyl)isoquinolinium bromide ((HCbiq)Br) with the corresponding metal salts. All these metal complexes were characterized by single crystal X-ray diffraction, elemental analyses, and IR. In complex **1**, the centrosymmetric binuclear Cu(Ⅱ) are bridged by four Cbiq molecules and each Cu(Ⅱ) ion is further coordinated to one water molecule. In complex **2**, the center Zn(Ⅱ) ion is coordinated to two unidentate Cbiq molecules and two water molecules. Complexes **3** and **4** have similar structures in which every two M(Ⅱ) ions are bridged by two Cbiq molecules and one hydroxo-O atom and the two peripheric M(Ⅱ) ions are further coordinated to two unidentate Cbiq molecules and one water molecule. Agarose gel electrophoresis (GE) studies on the cleavage of plasmid pBR322 DNA by complexes **1**-**4** indicated that complex **1** was capable of efficiently cleaving DNA under physiological conditions,

收稿日期:2022-05-19。收修改稿日期:2022-09-04。

国家自然科学基金(No.21874064,21871203)和广东省医学科学技术研究基金(No.A2021267)资助。

*通信联系人。E-mail:xuxuefei0731@163.com

most probably via an oxidative mechanism. Kinetic assay of complex **1** afforded the maximal catalytic rate constant k_{max} of 2.80 h^{-1} and Michaelis constant K_M of 3.22 $mmol \cdot L^{-1}$. Ethidium bromide (EB) displacement experiments indicated that complex **1** exhibited high DNA binding affinity toward calf-thymus (CT) DNA. The docking method was used to predict the CT DNA binding affinity of complex **1**, with the result that the binding free energy was −49.87 $kJ \cdot mol^{-1}$. CCDC: 2165985, **1**; 2165991, **2**; 2166081, **3**; 2166082, **4**.

Keywords: zwitterionic carboxylate ligand; transition metal complexes; crystal structures; DNA

0 Introduction

In the past decades, the metal complexes of carboxylates have been attracting considerable interest in biochemistry due to that they contain a bioactive group of carboxylate that has strong coordination ability and diverse coordination modes. Therefore, to date, a large number of metal complexes of carboxylates have been synthesized and some of them have exhibited promising biological activities, such as anti-tumor[1], antibacterial[2-3], hydrolytic or oxidative cleavage of DNA[4-5], DNA detection[6]. It is worth noting that more and more researchers used zwitterionic carboxylate ligands to construct complexes that have unique structures and potential applications in biological probes[7], ion exchange[8], and so on[9-10]. On the other hand, metal complexes that contain conjugated aromatic rings or with positively charged functional groups, such as quaternary ammonium, may have strong DNA binding abilities[11-12]. However, to date, the metal complexes based on the zwitterionic carboxylate ligands interacting with DNA have been reported rarely[13-15]. Therefore, further systematic investigation of these kinds of zwitterionic carboxylate complexes is necessary.

In an earlier study, we reported a water-soluble copper complex based on a zwitterionic carboxylate ligand, *N*-(4-carboxybenzyl)pyridinium bromide ((HCbp)Br)[16]. We found that this zwitterionic carboxylate complex showed moderate DNA-binding and cleaving activity. In addition, it is known that polypyridyl ligands, such as 2, 2′-bipyridine (bipy) and 1, 10-phenanthroline (phen), are chelating ligands for transition metal ions[17]. Because of the planar, rigid, and hydrophobic features of the polypyridyl ligands, their complexes have been used as intercalating or groove binding agents for DNA, which may contribute to DNA cleaving and anti-tumor activities[18]. Therefore, we decided to increase the size of the fused ring of the ligand which is based on quaternized isoquinoline instead of quaternized pyridinium to obtain complexes with stronger DNA interactions and better DNA-cleaving activities. With this thought in mind, herein we describe the synthesis of a new ligand of *N*-(4-carboxybenzyl)isoquinolinium bromide ((HCbiq)Br, Scheme 1) and its four metal complexes, $[Cu_2(Cbiq)_4(H_2O)_2]Br_4 \cdot 2H_2O$ (**1**), $[Zn(Cbiq)_2(H_2O)_2]Br_2 \cdot Cbiq \cdot H_2O$ (**2**), and $[M_3(Cbiq)_8(\mu\text{-}OH)_2(H_2O)_2](ClO_4)_4 \cdot 7H_2O$ (M=Co (**3**), Mn (**4**)). The interactions of complexes **1**-**4** with DNA were studied.

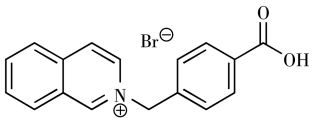

Scheme 1 Structures of (HCbiq)Br

1 Experimental

1.1 Generals

^1H and ^{13}C NMR spectra were recorded in DMSO-d_6 using a Varian Mercury 400 spectrometer and TMS as an internal reference. ESI-MS spectra were measured on Waters UPLC/Quattro Premier XE. IR spectra were recorded on a Nicolet Magna-IR 550. Elemental analyses for C, H, and N were performed on an EA1110 CHNS elemental analyzer. Agarose gel electrophoresis (GE) was conducted on a DYY-8C electrophoresis apparatus and DYCP-31DN electrophoresis chamber and detected on Alpha Hp 3400 fluorescence and visible light digital image analyzer. UV-Vis and fluorescence spectra were measured on a TU-1901 spectrophotometer and a HITACHI F-2500 spectrofluorimeter, respectively.

Calf-thymus (CT) DNA and plasmid pBR322 DNA were obtained from Sigma-Aldrich and Takara Chemical Co., respectively. Their solutions were prepared in 5 mmol·L^{-1} Tris-HCl buffer (5 mmol·L^{-1} NaCl, pH 7.0). The concentration of CT DNA was determined spectrophotometrically using the molar extinction coefficient of 13 200 L·mol^{-1}·cm^{-1} per base pair (bp) at 260 nm[19]. All the other chemicals and reagents were obtained from commercial sources and used without further purification. Buffer solutions were prepared in triply distilled deionized water.

1.2 Synthesis of (HCbiq)Br

To a solution of 4-(bromomethyl)benzoic acid (2.15 g, 10 mmol) in acetone (120 mL) was added drop slowly a solution of isoquinoline (1.3 g, 10 mmol) in acetone (30 mL) at room temperature. After stirring for 24 h, the white precipitates formed were collected through filtration and washed with ethyl acetate (5 mL) and ether (5 mL) to afford (HCbiq)Br (3.11 g, 75%). ^{1}H NMR (400 MHz, DMSO-d_6): δ 10.38 (s, H-9, 1H), 8.88 (dd, *J*=6.8, 1.2 Hz, H-1, 1H), 8.65 (d, *J*=6.8 Hz, H-2, 1H), 8.57 (d, *J*=8 Hz, H-7, 1H), 8.39 (d, *J*=8 Hz, H-4, 1H), 8.28-8.32 (m, H-5, 1H), 8.10-8.13 (m, H-6, 1H), 8.00 (d, *J*=8 Hz, H-13 and H-15, 2H), 7.71 (d, *J*=8 Hz, H-12 and H-16, 2H), 6.13 (s, H-10, 2H) (Fig.S1, Supporting information). ^{13}C NMR (100 MHz, DMSO-d_6): δ 166.6 (C-17), 150.4 (C-9), 138.7 (C-11), 137.2 (C-3), 137.1 (C-5), 134.8 (C-1), 131.3 (C-14) 131.3 (C-6), 130.6 (C-7), 129.9 (C-13 and C-15), 128.9 (C-12 and C-16), 127.3 (C-3 and C-4), 126.3 (C-2), 62.6 (C-10) (Fig.S2). ESI-MS *m/z*: 264.5 ([M−Br]$^+$). Main IR bands (KBr disc, cm^{-1}): 3 442(sb), 3 048(m), 3 008(m), 1 700 (s), 1 641(w), 1 608(w), 1 444(w), 1 398(w), 1 370(w), 1 222(m), 1 115(s), 1 066(s), 952(m), 822(m), 754(m), 538(m).

1.3 Synthesis of complexes 1-4

(HCbiq)Br (137.7 mg, 0.4 mmol) was dissolved in MeOH (4 mL), and the pH value of the solution was adjusted to 7.0 with 0.1 mol·L^{-1} NaOH solution. Then a solution of $CuSO_4$·$5H_2O$ (60 mg, 0.2 mmol) in MeOH (2 mL) was added. The resulting mixture was stirred for 1 h. The formed precipitates were collected by filtration, re-dissolved in H_2O (15 mL), and allowed to stand at ambient temperature for about one week to produce the blue crystals of complex **1** (120 mg, 76%). Elemental Anal. Calcd. for $C_{68}H_{60}Br_4N_4O_{12}Cu_2$(%): C 51.96, H 3.85, N 3.56. Found(%): C 52.09, H 3.99, N 3.72. Main IR bands (KBr disc, cm^{-1}): 3 443 (sb), 3 130 (sb), 1 610 (m), 1 445(m), 1 399 (s), 1 123 (s), 1 065 (s), 952 (m), 865 (m), 539 (m).

Complex **2** (98 mg, 69%) was prepared from (HCbiq)Br (137.7 mg, 0.4 mmol) and $ZnCl_2$ (27 mg, 0.2 mmol), using similar procedures as described for complex **1**. Elemental Anal. Calcd. for $C_{51}H_{45}Br_2N_3O_9Zn$ (%): C 57.29, H 4.24, N 3.93. Found(%): C 57.45, H 4.41, N 3.85. IR (KBr disc, cm^{-1}): 3 443 (sb), 3 065 (m), 1 616 (s), 1 565 (w), 1 396 (m), 1 369 (s), 1 151 (s), 1 070 (s), 954 (m), 860 (m), 811 (w), 544 (m).

(HCbiq)Br (137.7 mg, 0.4 mmol) was dissolved in MeOH (4 mL), and the pH value of the solution was adjusted to 7.0 with 0.1 mol·L^{-1} NaOH solution. Then a solution of $Co(ClO_4)_2$·$6H_2O$ (73.2 mg, 0.2 mmol) in MeOH (2 mL) was added. The resulting mixture was stirred at room temperature for 3 h and filtered to give a clear solution. Diethyl ether was allowed to diffuse into the filtrate. After standing at ambient temperature for two days, the formed pick crystals were collected by filtration, washed with Et_2O, and dried *in vacuo* to get complex **3** (81 mg, 56%). Elemental Anal. Calcd. for $C_{136}H_{124}Cl_4N_8O_{43}Co_3$(%): C 56.77, H 4.34, N 3.89. Found (%): C 56.56, H 4.26, N 3.71. IR (KBr disc, cm^{-1}): 3 444 (sb), 3 127 (w), 1 639 (w), 1 609 (m), 1 563(m), 1 443 (m), 1 403 (m), 1 264 (w), 1 120 (s), 1 066 (s), 995 (m), 951 (m), 865 (m), 819 (w), 563 (m), 540 (m), 515 (m).

Complex **4** (86 mg, 60%) was prepared from (HCbiq)Br (137.7 mg, 0.4 mmol) and $Mn(ClO_4)_2$·$6H_2O$ (73.2 mg, 0.2 mmol), using similar procedures as described for complex **3**. Elemental Anal. Calcd. for $C_{136}H_{124}Cl_4N_8O_{43}Mn_3$(%): C 57.01, H 4.36, N 3.91. Found(%): C 57.14, H 4.43, N 3.84. IR (KBr disc, cm^{-1}): 3 385 (sb), 1 638 (m), 1 611 (m), 1 566 (w), 1 403 (s), 1 151 (s), 1 072(s), 953 (w), 860 (m), 547 (m).

1.4 Structures determination for complexes 1-4

All the measurements were made on a Rigaku Mercury CCD X-ray diffractometer by using graphite

monochromated Mo $K\alpha$ (λ=0.071 073 nm). Crystals of complexes **1**-**4** were mounted with grease at the top of glass fiber. Cell parameters were refined by using the program CrystalClear. The collected data were reduced by using the program CrystalStructure while an absorption correction (multiscan) was applied. The structure was solved and refined using the SHELXTL program suite[20], equipped with XS[21] and XL programs[22]. Least-squares refinement routines were performed in refinement. Hydrogen atoms on carbon atoms were placed in calculated positions, and their coordinates and displacement parameters were constrained to ride on the carrier atom (C—H 0.097 nm, U_{iso}(H) =1.2U_{eq}(C) for alkyl H atoms; C—H 0.093 nm, U_{iso}(H)=1.2U_{eq}(C)) for aromatic H atoms. Hydrogen atoms on oxygen atoms were located from difference density maps. A summary of the key crystallographic information for complexes **1**-**4** is listed in Table 1.

CCDC: 2165985, **1**; 2165991, **2**; 2166081, **3**; 2166082, **4**.

Table 1 Crystallographic data for complexes 1-4

Parameter	1	2	3	4
Molecular formula	$C_{68}H_{60}Br_4N_4O_{12}Cu_2$	$C_{51}H_{45}Br_2N_3O_9Zn$	$C_{136}H_{124}Cl_4N_8O_{43}Co_3$	$C_{136}H_{124}Cl_4N_8O_{43}Mn_3$
Formula weight	1 571.92	1 069.09	2 877.02	2 865.05
Crystal system	Monoclinic	Monoclinic	Rhombohedral	Rhombohedral
Space group	*C*2/*c*	$P2_1$	$R\bar{3}$	$R\bar{3}$
a / nm	3.028 31(11)	1.012 41(12)	3.616 12(11)	3.661 23(12)
b / nm	1.710 53(13)	2.720 92(13)	3.616 12(11)	3.661 23(12)
c / nm	1.379 12(12)	2.053 81(12)	3.079 59(14)	3.125 32(18)
β / (°)	102.121(3)	91.081(3)		
V / nm^3	6.984 6(8)	5.656 6(8)	34.875(2)	36.281(3)
Z	4	4	9	9
T / K	291(2)	291(2)	291(2)	291(2)
D_c / (g·cm^{-3})	1.495	1.255	1.233	1.180
μ / mm^{-1}	2.958	1.897	0.463	0.371
Total reflection	31 641	42 020	84 481	92 574
$2\theta_{max}$ / (°)	52.00	52.00	52.00	52.00
Unique reflection	6 851 (R_{int}=0.069 1)	20 940 (R_{int}=0.018 6)	15 113 (R_{int}=0.073 3)	15 797 (R_{int}=0.066 8)
Observed reflection [$I>2\sigma(I)$]	4 423	16 594	10 376	11 483
Number of parameters	424	1 271	912	912
R[a]	0.061 2	0.050 5	0.063 9	0.058 6
wR[b]	0.133 2	0.123 3	0.138 9	0.110 0
GOF[c]	1.072	1.024	1.071	1.075
$(\Delta\rho)_{max}$, $(\Delta\rho)_{min}$ / (e·nm^{-3})	780, −424	441, −307	295, −317	295, −251

[a] $R=\sum||F_o|-|F_c||/|F_o|$; [b] $wR=[\sum w(F_o^2-F_c^2)^2/\sum w(F_o^2)^2]^{1/2}$; [c] GOF=$[\sum w(F_o^2-F_c^2)^2/(n-p)]^{1/2}$, where n is the number of reflections and p is the total numbers of parameters refined.

1.5 DNA cleavage

The cleavage experiments were conducted by using methods similar to those described previously[23-25]. Specifically, a mixture of pBR322 DNA (0.5 g·L^{-1}, 0.7 μL) and each of complexes **1**-**4** was diluted with 5 mmol·L^{-1} Tris-HCl buffer (5 mmol·L^{-1} NaCl, pH 7.0) to 16 μL and incubated at 37 ℃ for 5 h. The reaction was quenched by adding loading buffer containing 0.035% bromophenol blue, 36% glycerol, 30 mmol·L^{-1} EDTA, and 0.05% xylene cyanol FF. The solution was then loaded on 1% agarose gel containing EB (ethidium bromide, 1.0 mg·L^{-1}) and analyzed with electrophoresis in Tris-acetate-EDTA (TAE) buffer (pH 8.0). Bands were visualized by UV light and photographed.

The kinetics for the DNA cleavage was investigated at 37 ℃ for different intervals of time, by varying the

concentrations of complex **1** in 5 mmol·L^{-1} Tris-HCl buffer (5 mmol·L^{-1} NaCl, pH 7.0)[23-25]. The percentage of the supercoiled DNA form was determined and plotted against time for each concentration of complex **1**. The data were fitted with a single-exponential curve (pseudo-first-order kinetics) to give the k_{obs} values. The k_{obs} values were then plotted versus the concentrations (c_1) of complex **1** (Eq.**1**), allowing the determination of the corresponding maximal first-order rate constant k_{max} and Michaelis constant K_M.

$$k_{obs}=k_{max}c_1/(K_M+c_1) \quad (1)$$

For mechanistic investigations, inhibition reactions were carried out in the presence of DMSO (1.0 mol·L^{-1}), MeOH (1.0 mol·L^{-1}), NaN_3 (0.1 mol·L^{-1}), KI (0.1 mol·L^{-1}), and EDTA (0.1 mol·L^{-1}), followed by the addition of complex **1**.

1.6 DNA binding experiment

EB displacement experiments of (HCbiq)Br and complexes **1-4** were performed by keeping the concentrations of CT DNA and EB constant, while gradually increasing the concentrations of (HCbiq)Br or each of the metal complexes. Thus, to a solution of CT DNA (2.10 μmol·L^{-1}) and EB (2.63 μmol·L^{-1}) in 5 mmol·L^{-1} Tris-HCl (5 mmol·L^{-1} NaCl, pH 7.0) were added aliquots of a solution of each compound containing CT DNA (2.10 μmol·L^{-1}) and EB (2.63 μmol·L^{-1}) in the same buffer. The corresponding fluorescence spectra were measured (λ_{ex}=510 nm) until saturation was observed. The apparent binding constant (K_a) was obtained by analyzing the relative fluorescence intensity (I/I_0) as a function of the concentration of each complex[26].

1.7 Molecular docking

The molecule structure of complex **1** was constructed and optimized using Molecular Operating Environment (MOE) package[27], while the 3D structure of DNA (PDB ID: 453D) was constructed and optimized by the Chimera package[28]. The initial structures of DNA with compound **1** were manually built by molecular docking in MOE to give the binding energies[29]. The visual analysis of binding modes was obtained in the force field by Python molecule (PyMOL)[30].

2 Results and discussion

2.1 Synthesis of (HCbiq)Br and complexes 1-4

The synthetic route of (HCbiq)Br and complexes **1-4** is shown in Scheme 2. Thus, the reaction of isoquinoline with 4-(bromomethyl)benzoic acid in acetone afforded (HCbiq)Br in 75% yield. Treatment of (HCbiq)Br with 1/2 Equiv. of the corresponding metal salts gave complexes **1-4** in 56%-76% yields.

(HCbiq)Br was characterized by ^{1}H NMR, ^{13}C NMR, ESI-MS, elemental analyses, and IR, while the structures of complexes **1-4** were confirmed by single-crystal X-ray crystallography, elemental analyses, and IR. The elemental analyses of (HCbiq)Br and complexes **1-4** were consistent with their chemical formula, and the ^{1}H NMR and ^{13}C NMR spectra of (HCbiq)Br were also in full agreement with the given structures. Complexes **1-4** were further characterized by single-crystal X-ray crystallography.

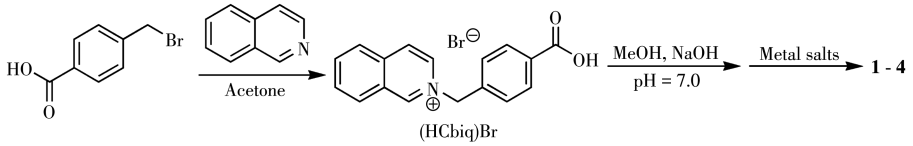

Scheme 2 Synthesis of (HCbiq)Br and complexes **1-4**

2.2 Crystal structures of complexes 1-4

2.2.1 Structure of complex 1

Complex **1** crystallizes in the monoclinic space group *C*2/*c*. In complex **1**, each asymmetric unit consists of half a $[Cu_2(Cbiq)_4(H_2O)_2]^{2+}$ dication, two Br^- anions, and three H_2O molecules (two of them having 0.3 occupancies, one of them having 0.4 occupancies). As depicted in Fig. 1, the centrosymmetric binuclear coppers are bridged by four Cbiq molecules, and each copper ion is further coordinated to one water molecule, thereby forming a paddle-wheel structure with four carboxylate bridges. There is a center symmetry

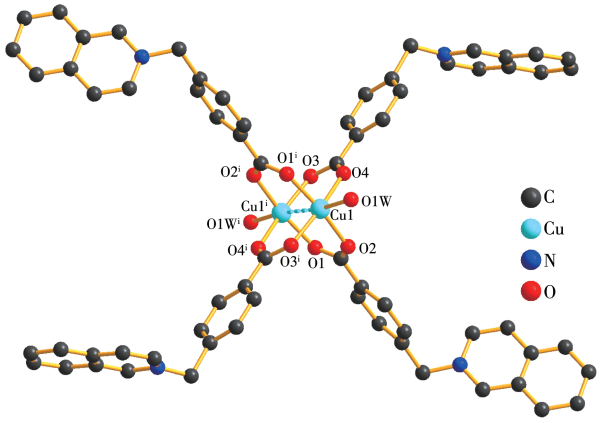

All the hydrogen atoms are omitted for clarity; Symmetry code: ⁱ 2−*x*, −*y*, 2−*z*

Fig.1 Perspective view for the structure of $[Cu_2(Cbiq)_4(H_2O)_2]^{2+}$ dication in **1**

point at the center of the bond Cu1⋯Cu1ⁱ with a bond length of 0.261 4(14) nm. The selected bond distances and angles for complex **1** are shown in Table 2.

2.2.2 Structure of complex **2**

Complex **2** crystallizes in the monoclinic space group $P2_1$ and the asymmetric unit consists of two $[Zn(Cbiq)_2(H_2O)_2]^{2+}$ dications, two Cbiq molecules, ten Br^- anions (three of them having 0.3 occupancies, four of them having 0.4 occupancies and three of them having 0.5 occupancies), and five H_2O molecules (each of them having 0.4 occupancies). As depicted in Fig.2, the center Zn ion is coordinated by two H_2O molecules and two O atoms of carboxylate from two unidentate Cbiq molecules, thereby forming a distorted tetrahedron coordination geometry. The selected bond distances and angles for complex **2** are shown in Table 3.

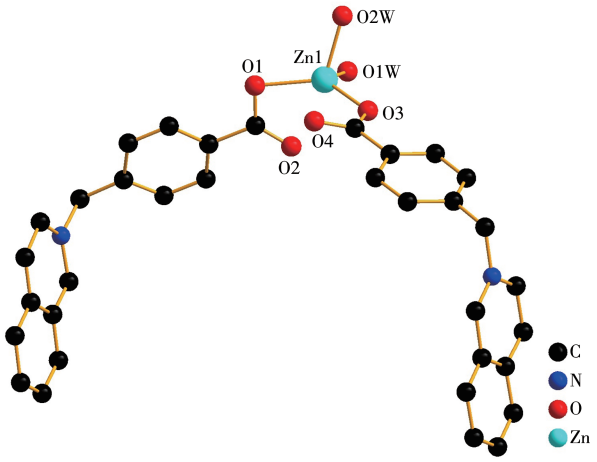

All the hydrogen atoms are omitted for clarity

Fig.2 Perspective view for the structure of $[Zn(Cbiq)_2(H_2O)_2]^{2+}$ dication in **2**

2.2.3 Structure of complexes **3** and **4**

Complexes **3** and **4** all crystallize in the trigonal

Table 2 Selected bond lengths (nm) and angles (°) for complex 1

Cu1—O1ⁱ	0.194 2(4)	Cu1—O4	0.198 3(4)	Cu1—O2	0.198 6(4)
Cu1—O3ⁱ	0.199 8(4)	Cu1—O1W	0.215 4(4)	Cu1—Cu1ⁱ	0.261 4(14)
O1ⁱ—Cu1—O4	88.85(17)	O1ⁱ—Cu1—O2	168.99(16)	O4ⁱ—Cu1—O2ⁱ	91.64(16)
O1ⁱ—Cu1—O3ⁱ	89.65(16)	O4—Cu1—O3ⁱ	169.83(17)	O2—Cu1—O3ⁱ	87.94(16)
O1ⁱ—Cu1—O1W	91.69(16)	O4—Cu1—O1W	95.30(15)	O2—Cu1—O1W	99.21(16)
O3ⁱ—Cu1—O1W	94.80(16)	O1ⁱ—Cu1—Cu1ⁱ	83.30(12)	O4—Cu1—Cu1ⁱ	80.89(12)
O2—Cu1—Cu1ⁱ	85.91(12)	O3ⁱ—Cu1—Cu1ⁱ	88.94(17)	O1W—Cu1—Cu1ⁱ	173.74(11)

Symmetry code: ⁱ 2−*x*, −*y*, 2−*z*.

Table 3 Selected bond lengths (nm) and angles (°) for complex 2

Zn1—O1	0.206 1(3)	Zn1—O3	0.192 4(3)	Zn2—O6	0.202 9(3)
Zn2—O8	0.220 2(3)	Zn1—O1W	0.199 5(3)	Zn1—O2W	0.197 8(3)
Zn2—O3W	0.198 8(3)	Zn2—O4W	0.193 4(3)		
O3—Zn1—O2W	98.71(14)	O3—Zn1—O1W	112.49(14)	O2W—Zn1—O1W	89.26(13)
O3—Zn1—O1	133.07(13)	O2W—Zn1—O1	111.42(13)	O1W—Zn1—O1	103.30(13)
O4W—Zn2—O3W	95.95(13)	O4W—Zn2—O6	106.37(13)	O3W—Zn2—O6	101.11(13)
O4W—Zn2—O8	96.79(12)	O3W—Zn2—O8	104.12(12)	O6—Zn2—O8	143.53(12)

space group $R\bar{3}$ and the asymmetric unit consists of half a $[M_3(Cbiq)_8(\mu\text{-}OH)_2(H_2O)_2]^{2+}$ dication (M=Co (**3**), Mn (**4**)), two ClO_4^- anions, nine H_2O molecules (two of them having 0.5 occupancies, five of them having 0.4 occupancies, one of them having 0.33 occupancies and one of them having 0.17 occupancies). Because complexes **3** and **4** have similar $[M_3(Cbiq)_8(\mu\text{-}OH)_2(H_2O)_2]^{2+}$ dication structures in which every two M(Ⅱ) ions are bridged by two Cbiq molecules and one hydroxo-O atom and the two peripheric M(Ⅱ) ions further coordinate to two unidentate Cbiq molecules and one H_2O molecule, only the perspective view of the molecular structure of complex **3** is depicted in Fig.3. The selected bond distances and angles for complexes **3** and **4** are listed in Table 4. The similar structure of complex **4** is shown in Fig.S3.

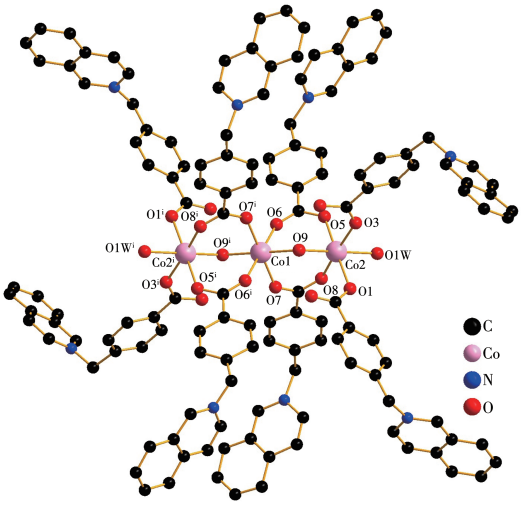

All the hydrogen atoms are omitted for clarity; Symmetry code: i 1−*x*, 2−*y*, −*z*

Fig.3 Perspective view for the structure of $[Co_3(Cbiq)_8(\mu\text{-}OH)_2(H_2O)_2]^{4+}$ cation in **3**

Table 4 Selected bond lengths (nm) and angles (°) for complexes 3 and 4

3					
Co1—O7^i	0.206 3(2)	Co1—O7	0.206 3(2)	Co1—O6^i	0.207 0(2)
Co1—O6	0.207 0(2)	Co1—O9^i	0.211 0(2)	Co1—O9	0.211 0(2)
Co2—O8	0.201 9(2)	Co2—O3	0.209 3(2)	Co2—O5	0.209 8(2)
Co2—O9	0.212 0(2)	Co2—O1	0.214 3(2)	Co2—O1W	0.216 8(2)
O7^i—Co1—O7	180.00(8)	O7^i—Co1—O6^i	90.76(8)	O7—Co1—O6^i	89.24(8)
O7^i—Co1—O6	89.24(8)	O7—Co1—O6	90.76(8)	O6i—Co1—O6	180.00(11)
O7^i—Co1—O9^i	92.49(8)	O7—Co1—O9^i	87.51(8)	O6i—Co1—O9^i	92.01(8)
O6—Co1—O9^i	87.99(8)	O7^i—Co1—O9	87.51(8)	O7—Co1—O9	92.49(8)
O6^i—Co1—O9	87.99(8)	O6—Co1—O9	92.01(8)	O9^i—Co1—O9	180.00(13)
O8—Co2—O3	173.80(8)	O8—Co2—O5	89.54(8)	O3—Co2—O5	88.81(8)
O8—Co2—O9	98.06(8)	O3—Co2—O9	88.03(8)	O5—Co2—O9	94.64(8)
O8—Co2—O1	87.95(8)	O3—Co2—O1	93.38(8)	O5—Co2—O1	176.09(8)
O9—Co2—O1	88.68(8)	O8—Co2—O1W	86.70(9)	O3—Co2—O1W	87.31(8)
O5—Co2—O1W	89.58(9)	O9—Co2—O1W	173.65(9)	O1—Co2—O1W	87.29(9)
4					
Mn1—O7	0.209 4(16)	Mn1—O7^i	0.209 4(16)	Mn1—O6^i	0.209 5(16)
Mn1—O6	0.209 5(16)	Mn1—O9	0.214 5(15)	Mn1—O9^i	0.214 5(15)
Mn2—O8	0.204 7(16)	Mn2—O5	0.212 3(17)	Mn2—O3	0.212 7(17)
Mn2—O9	0.215 4(15)	Mn2—O1	0.217 6(16)	Mn2—O1W	0.219 2(16)
O7—Mn1—O7^i	180.00(10)	O7—Mn1—O6^i	89.33(6)	O7^i—Mn1—O6^i	90.67(6)
O7—Mn1—O6	90.67(6)	O7^i—Mn1—O6	89.33(6)	O6^i—Mn1—O6	180.0
O7—Mn1—O9	92.29(6)	O7^i—Mn1—O9	87.71(6)	O6^i—Mn1—O9	87.84(6)
O6—Mn1—O9	92.16(6)	O7—Mn1—O9^i	87.71(6)	O7^i—Mn1—O9^i	92.29(6)
O6^i—Mn1—O9^i	92.16(6)	O6—Mn1—O9^i	87.84(6)	O9—Mn1—O9^i	180.0
O8—Mn2—O5	89.57(7)	O8—Mn2—O3	173.99(6)	O5—Mn2—O3	88.73(7)

Continued Table 4

O8—Mn2—O9	97.99(6)	O5—Mn2—O9	94.55(6)	O3—Mn2—O9	87.89(6)
O8—Mn2—O1	87.90(6)	O5—Mn2—O1	176.18(7)	O3—Mn2—O1	93.50(7)
O9—Mn2—O1	88.63(6)	O8—Mn2—O1W	86.87(6)	O5—Mn2—O1W	89.69(7)
O3—Mn2—O1W	87.35(7)	O9—Mn2—O1W	173.55(7)	O1—Mn2—O1W	87.32(7)

Symmetry codes: [i] 1−*x*, 2−*y*, −*z* for **3**; [i] 1−*x*, 2−*y*, −*z* for **4**.

2.3 Cleavage of pBR322 DNA

It is known that many metal complexes are capable of catalyzing the cleavage of DNA[31]. We investigated the cleaving activities of complexes **1** - **4** toward pBR322 DNA. Fig. 4 shows the GE patterns for the cleavage of pBR322 DNA by complexes **1**-**4** at pH 7.0 and 37 ℃. It can be seen that the conversion of the supercoiled DNA (CCC) form (Form Ⅰ) into the open circular (OC) form (Form Ⅱ) was apparent. The DNA-cleaving efficiency decreased in the order of complex **1** (Lane 3) ≫ **2** (Lane 4) ≈ **3** (Lane 5) ≈ **4** (Lane 6). Of the four complexes, complex **1** was the most active and therefore its DNA-cleaving activity was further explored.

Firstly, we carried out the concentration - dependent DNA cleavage by complex **1** (Fig. 5). It can be seen that complex **1** was capable of efficiently converting pBR322 DNA into OC form and that the cleaving activity increased with the concentration of complex **1** (Lanes 2-7). When the concentration of complex **1** was about 0.5 mmol·L^{-1}, almost all of Form Ⅰ was converted to Form Ⅱ. It should be noted that neither (HCbiq)Br (Lane 8) nor $CuSO_4$ (Lane 9) showed any obvious cleaving activity. Such concentration dependence experiments lent strong support that complex **1** catalyzed the cleavage.

Secondly, to gain insight into the cleaving activity of complex **1**, the kinetics of pBR322 DNA degradation was studied. Fig. 6a shows that the extent of supercoiled DNA cleavage into Form Ⅱ varied exponentially with the reaction time (0.5 mmol·L^{-1}), giving pseudo-first - order kinetics with a rate constant of (0.494±0.032) h^{-1}. The saturation kinetics profile (Fig.6b) gave the k_{max} and K_M obtained from the saturation ((2.80±0.97) h^{-1} and (3.22±0.76) mmol·L^{-1}) for complex **1**. Thus, the catalytic efficiency (k_{max}/K_M) was 0.88 L·mmol^{-1}·h^{-1} for complex **1**. In particular, complex **1** could catalyze the cleavage at a rate acceleration of about 10^8 fold over uncatalyzed cleavage of supercoiled

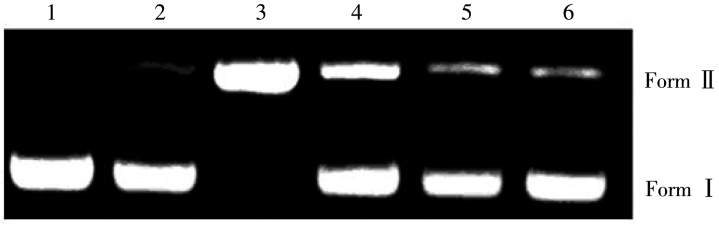

Lane 1, DNA alone; Lane 2, DNA+(HCbiq)Br; Lanes 3-6, DNA in the presence of complexes **1**-**4**, respectively

Fig.4 Agarose GE patterns for the cleavage of pBR322 DNA by complexes **1**-**4** (1 mmol·L^{-1}) and (HCbiq)Br (4 mmol·L^{-1}) in 5 mmol·L^{-1} Tris-HCl (5 mmol·L^{-1} NaCl, pH 7.0) at 37 ℃ (5 h)

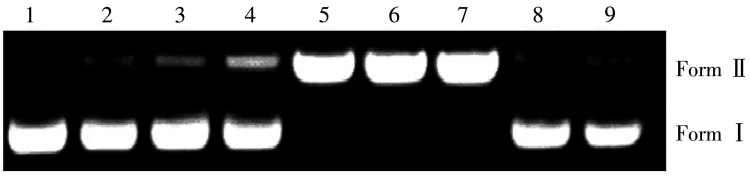

Lane 1, DNA alone; Lanes 2−7, DNA+complex **1** at the concentrations of 0.05, 0.1, 0.2, 0.5, 0.75, and 1.0 mmol·L^{-1}, respectively; Lane 8, DNA+(HCbiq)Br (4 mmol·L^{-1}); Lane 9, DNA+$CuSO_4$ (2 mmol·L^{-1})

Fig.5 Agarose GE patterns for the cleavage of pBR322 DNA by complex **1** of increasing concentrations in 5 mmol·L^{-1} Tris-HCl (5 mmol·L^{-1} NaCl, pH 7.0) at 37 ℃ (5 h)

DNA cleavage (k=3.6×10^{-8} h^{-1} for cleavage of a phosphodiester bond in double-stranded DNA under physiological condition)[32-34].

Thirdly, to gain further insight into the cleaving activity of complex **1**, its mechanism of action toward the cleavage of pBR322 DNA was investigated. It is known that nucleic acid can be cleaved through either an oxidative or hydrolytic pathway. In general, oxidative cleavage of plasmid DNA may lead to the formation of reactive singlet oxygen ($^1O_2$), hydrogen peroxide (H_2O_2), and/or hydroxyl radical (·OH) species. These species contain a photo or redox active center, which causes damage to the sugar and/or base[34-35]. Therefore, to distinguish the probable mechanism of action of complex **1**, we conducted the cleavage reactions in the presence of hydroxyl radical scavengers DMSO and MeOH, singlet oxygen scavenger NaN_3, hydrogen peroxide scavenger KI and metal ion-chelating agent EDTA[36] (Fig.7). As a result, EDTA (Lane 6) efficiently inhibited DNA cleavage, indicating that complex **1** was obligatory in DNA cleavage reaction. When DMSO (Lane 3) and MeOH (Lane 4) were added to the reaction mixture, no significant influence on the DNA cleavage was observed, strongly suggesting that hydroxyl radical was not involved in the DNA cleavage. In the presence of NaN_3 (Lane 7), the DNA cleavage was significantly inhibited, suggesting that singlet oxygen was likely to be the reactive species responsible for the nuclease activity[37]. Similarly, in the presence of KI (Lane 5), the cleavage was repressed, suggesting that H_2O_2 might be the reactive species in the cleavage process. Taken together, these results strongly suggest that DNA cleavage by complex **1** proceeds via an oxidative mechanism[38]. Thus, the proposed mechanism may be that the copper centers strongly bind O_2 to form reactive oxygen species (ROS), such as singlet oxygen and superoxide,

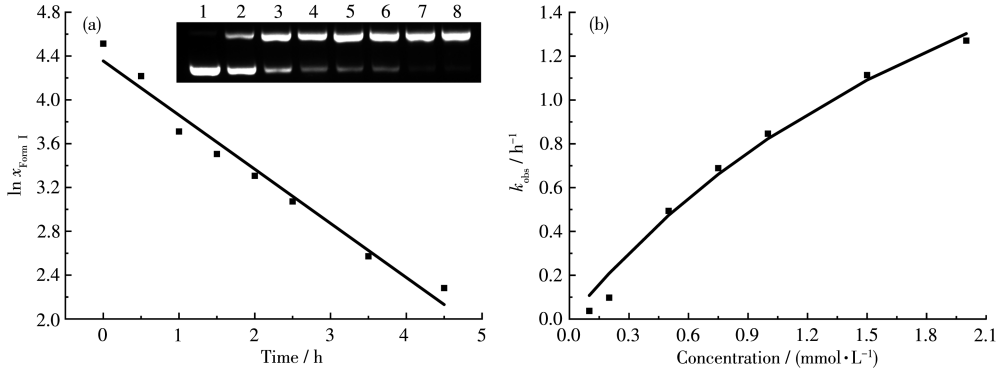

$x_{Form\ I}$ is the percentage of supercoiled DNA (Form Ⅰ); Inset: agarose GE patterns of the time-variable reaction products; Lane 1, DNA alone; Lanes 2-8, reaction time was 0.5, 1, 1.5, 2, 2.5, 3.5, and 4.5 h, respectively

Fig.6 (a) Time course of pBR322 DNA cleavage promoted by complex **1** (0.5 mmol·L^{-1}) in 5 mmol·L^{-1} Tris-HCl (5 mmol·L^{-1} NaCl, pH 7.0) at 37 ℃; (b) Saturation kinetics plot of k_{obs} versus the concentration of complex **1**

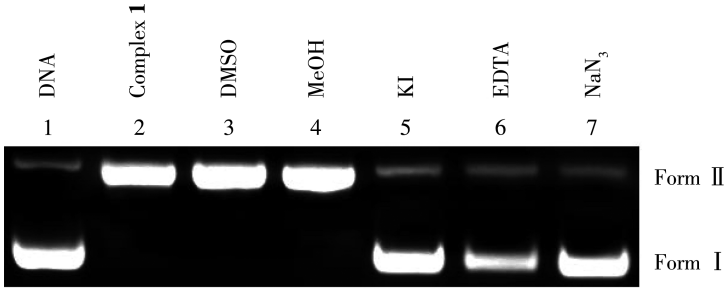

Lane 1, DNA alone; Lane 2, DNA+**1**

Fig.7 Agarose GE patterns for the cleavage of pBR322 DNA by complex **1** (1 mmol·L^{-1}) at pH 7.0 and 37 ℃ for 5 h, in the presence of DMSO (1 mol·L^{-1}, Lane 3), MeOH (1 mol·L^{-1}, Lane 4), KI (0.1 mol·L^{-1}, Lane 5), EDTA (0.1 mol·L^{-1}, Lane 6), NaN_3 (0.1 mol·L^{-1}, Lane 7)

which can further activate the cleavage of supercoiled DNA to form nicked DNA[39].

2.4 DNA binding

It is widely recognized that DNA binding is a critical step for DNA cleavage in most cases. Thus, we estimated the binding affinities of complexes **1**-**4** by means of EB displacement experiments. EB emits intense fluorescent light in the presence of DNA due to its strong intercalation between the adjacent DNA base pairs. Competitive binding of other drugs to DNA leads to the displacement of bound EB and a decrease in fluorescence intensity[40]. Under the measuring conditions, (HCbiq)Br and complexes **1**-**4** induced decreases in the fluorescence intensity (FI) of EB (Fig.S10-S19), indicating that they were capable of substituting EB bound to CT DNA. Their binding constants were obtained by analyzing the relationship between the relative fluorescence intensity and the concentrations of each complex (Table 5). As a result, complex **1** had the highest affinity with the binding constant being (8.63±3.82)×10^5 L·mol^{-1}, 10-100 fold higher than those of complexes **2**-**4** and (HCbiq)Br, which was consistent with their DNA cleaving activities.

2.5 Molecular docking

Table 5 Binding constants (K_a) with CT DNA of (HCbiq)Br and complexes 1-4*

Compound	K_a / (L·mol^{-1})
(HCbiq)Br	(4.59±0.88)×10^3
1	(8.63±3.82)×10^5
2	(3.16±0.51)×10^3
3	(6.86±1.38)×10^4
4	(2.02±1.02)×10^4

* Measured by means of EB displacement experiments, in 5 mmol·L^{-1} Tris-HCl (5 mmol·L^{-1} NaCl, pH 7.0) at room temperature.

Molecule simulation is an efficient way to predict the binding mode and the interaction region[41]. Molecular docking simulates the bonding form between the molecule and target DNA. The negative values of the binding energy of docked compounds suggest that the compounds bind to DNA strands. The binding free energy of complex **1** was −49.87 kJ·mol^{-1}. Fig.8 shows that complex **1** binds DNA through hydrogen bonds and π-π stacking between aromatic rings from bases of CT DNA and benzene rings from complex **1**. Complex **1** binds to the large groove of CT DNA and intercalates with it, forming eight aromatic centers (0.35-0.56 nm) and two hydrogen bonds (0.29-0.34 nm). The hydrophobic interaction between CT DNA and complex **1** was also formed, which was not shown in the figure. Thus, computer-aided molecular docking studies show there are many interactions between CT DNA and complex **1**. It has been reported that most synthesized metal complexes could bind to DNA with intercalation mode[42-43], which would affect the stability of DNA, thus exhibiting DNA cleavage capacity.

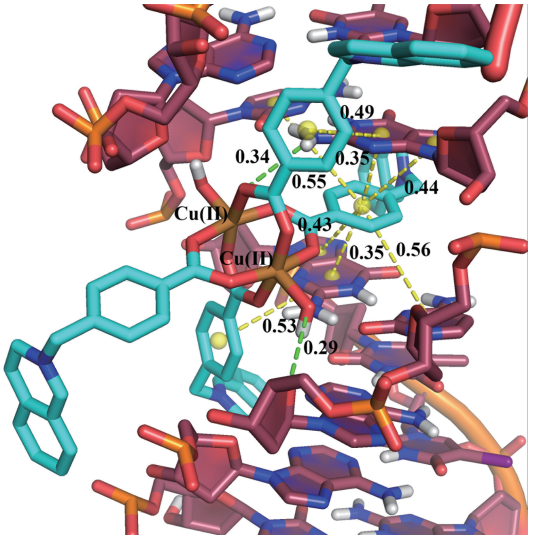

Complex **1** is displayed by cyan sticks, while CT DNA is by salmon cartoons; aromatic ring centers are denoted by yellow balls, π-π stacking interactions by yellow dashes, and hydrogen bonds by green dashes

Fig.8 Interaction modes between complex **1** and CT DNA

3 Conclusions

In summary, the new ligand of (HCbiq)Br and its four metal complexes have been synthesized and fully characterized. The efficiency of (HCbiq)Br and its metal complexes in promoting the cleavage of DNA was monitored by the use of agarose GE. Kinetic assays indicated that complex **1** was capable of efficiently cleaving plasmid pBR322 DNA, most probably through an oxidative mechanistic pathway. Molecular docking exposed the binding mode of complex **1** with DNA.

The results presented in this study highlight the fact that zwitterionic carboxylate metal complexes

exhibit biological activities. Efforts aimed at developing diverse zwitterionic carboxylate metal complexes are currently in progress with a view toward the design of new synthetic nucleases with promising antitumor activity.

Acknowledgments: This work was financially supported by the National Natural Science Foundation of China (Grants No. 21874064, 21871203), and the Medical Scientific Research Foundation of Guangdong Province of China (Grant No. A2021267).

Supporting information is available at http://www.wjhxxb.cn

References:

[1]Waseem D, Butt A F, Haq I U, Bhatti M H, Khan G M. Carboxylate Derivatives of Tributyltin(Ⅳ) Complexes as Anticancer and Antileishmanial Agents. *DARU*, **2017**,**25**(1):8

[2]Fudulu A, Olar R, Maxim C, Scăeţeanu G V, Bleotu C, Matei L, Chifiriuc M C, Badea M. New Cobalt(Ⅱ) Complexes with Imidazole Derivatives: Antimicrobial Efficiency against Planktonic and Adherent Microbes and *In Vitro* Cytotoxicity Features. *Molecules*, **2020**, **26**(1):55

[3]Sirajuddin M, Ali S, Mckee V, Matin A. Synthesis, Characterization and Biological Screenings of 5-Coordinated Organotin(Ⅳ) Complexes Based on Carboxylate Ligand. *J. Mol. Struct.*, **2020**,**1206**:127683

[4]Begum R, Rehman M U, Shahid K, Haider A, Iqbal M, Tahir M N, Ali S. Synthesis, Structural Elucidation, DNA-Binding and Biological Activity of Nickel(Ⅱ) Mixed Ligand Carboxylate Complexes. *J. Mol. Struct.*, **2021**,**1242**:130801

[5]Bhattacharjee M, Boruah S R, Purkayastha R, Ganguly R, Nath P. Synthesis, Characterization, DNA Binding Ability, *In Vitro* Cytotoxicity, Electrochemical Properties and Theoretical Studies of Copper(Ⅱ) Carboxylate Complexes. *Inorg. Chim. Acta*, **2021**,**518**:120235

[6]Zhao H Q, Yang S P, Ding N N, Qin L, Qiu G H, Chen J X, Zhang W H, Chen W H, Hor T S A. A Zwitterionic 1D/2D Polymer Co-crystal and Its Polymorphic Sub-components: A Highly Selective Sensing Platform for HIV ds-DNA Sequences. *Dalton Trans.*, **2016**, **45**(12):5092-5100

[7]Qin L, Lin L X, Fang Z P, Yang S P, Qiu G H, Chen J X, Chen W H. A Water-Stable Metal-Organic Framework of a Zwitterionic Carboxylate with Dysprosium: A Sensing Platform for Ebolavirus RNA Sequences. *Chem. Commun.*, **2016**,**5**(1):132-135

[8]An W, Aulakh D, Zhang X, Verdegaal W, Dunbar K R, Wriedt M. Switching of Adsorption Properties in a Zwitterionic Metal-Organic Framework Triggered by Photogenerated Radical Triplets. *Chem. Mater.*, **2016**,**28**(21):7825-7832

[9]Wang K M, Tang H J, Zhang D H, Ma Y L, Wang Y N. Selective and Recyclable Sensing of Aqueous Phase 2, 4, 6-Trinitrophenol (TNP) Based on Cd (Ⅱ) Coordination Polymer with Zwitterionic Ligand. *Crystals*, **2018**,**8**(12):456

[10]Ma Y L, Du L, Zhao Q H. Synthesis, Crystal Structure, Luminescent and Magnetic Properties of Lanthanide Coordination Polymers Based on a Zwitterionic Polycarboxylate Ligand. *Inorg. Chem. Commun.*, **2017**,**77**:1-5

[11]Devi C S, Thulasiram B, Aerva R R, Nagababu P. Recent Advances in Copper Intercalators as Anticancer Agents. *J. Fluoresc.*, **2018**,**28**(5):1195-1205

[12]Elif E Ş, Topkaya C G, Göktürk T, Gup R. 含季铵盐的芳酰腙配体的铜(Ⅱ)配合物的合成和表征:体外DNA键合和核酸酶活性. 无机化学学报, **2020**,**36**(7):1333-1343
Elif E Ş, Topkaya C G, Göktürk T, Gup R. Synthesis and Characterization of Copper(Ⅱ) Complexes with Aroylhydrazone Ligands Containing Quaternary Ammonium Salts: *In Vitro* DNA Binding and Nuclease Activity. *Chinese J. Inorg. Chem.*, **2020**,**36**(7):1333-1343

[13]Chen M, Tang X Y, Chen M Z, Chen J X, Chen W H. Lanthanide-Based Polymers with Charged Ligand Backbones: Triple-Stranded Chain Structures and Their DNA Cleavage Studies. *Aust. J. Chem.*, **2015**,**68**(3):493-499

[14]Chen J X, Lin W E, Chen M Z, Zhou C Q, Lin Y L, Chen M, Jiang Z H, Chen W H. Synthesis, Characterization and Potent DNA-Cleaving Activity of Copper(Ⅱ)-Complexed Berberine Carboxylate. Bioorg. *Med. Chem. Lett.*, **2012**,**22**(23):7056-7059

[15]Chen J X, Lin W E, Zhou C Q, Yau L F, Wang J R, Wang B, Chen W H, Jiang Z H. Synthesis, Crystal Structures and Biological Evaluation of Water-Soluble Zinc Complexes of Zwitterionic Carboxylates. *Inorg. Chim. Acta*, **2011**,**376**(1):389-395

[16]Chen J X, Lin W E, Chen M, Que F C, Tao L, Cen X L, Zhou Y M, Chen W H. Synthesis and DNA Photocleaving Activities of Ancillary Ligand-Containing Zinc Complexes of Quaternized Carboxylates. *Inorg. Chim. Acta*, **2014**,**409**:195-201

[17]Deo K M, Pages B J, Ang D L, Gordon C P, Aldrich-Wright J R. Transition Metal Intercalators as Anticancer Agents-Recent Advances. *Int. J. Mol. Sci.*, **2016**,**17**(12):1818-1835

[18]Chen M, Tang X Y, Yang S P, Li H H, Zhao H Q, Jiang Z H, Chen J X, Chen W H. Five Water-Soluble Zwitterionic Copper(Ⅱ)-Carboxylate Polymers: Role of Dipyridyl Coligands in Enhancing the DNA-Binding, Cleaving and Anticancer Activities. *Dalton Trans.*, **2015**,**44**(29):13369-13377

[19]Reichmann M E, Rice S A, Thomas C A, Doty P. A Further Examination of the Molecular Weight and Size of Desoxypentose Nucleic Acid. *J. Am. Chem. Soc.*, **1954**,**76**(11):3047-3053

[20]Sheldrick G M. *SHELXTL*, *Version* 5.1. Bruker AXS Inc., Madison, Wisconsin, USA, **1997**.

[21]Sheldrick G M. *SHELXS*-97, *Program for the Solution of Crystal Structure*. University of Göttingen, Germany, **1997**.

[22]Sheldrick G M. *SHELXL*-97, *Program for the Refinement of Crystal Structures*. University of Göttingen, Germany, **1997**.

[23]Zhou C Q, Lin Y L, Chen J X, Wang L S, Yang N N, Zeng W, Chen

W H. Facile Synthesis of a Dimeric Dipyrrole-Polyamide and Synergetic DNA-Cleaving Activity of Its Cu(Ⅱ) Complex. *Bioorg. Med. Chem. Lett.*, **2012**,**22**(18):5853-5856

[24]Zhou C Q, Lin Y L, Chen J X, Chen W H. Synergetic DNA-Cleaving Activities of the Metal Complexes of a Polyether-Tethered Pyrrole-polyamide Dimer. *Chem. Biodivers.*, **2012**,**9**(6):1125-1132

[25]Chen M Z, Chen M, Zhou C Q, Lin W E, Chen J X, Chen W H, Jiang Z H. Synthesis, Crystal Structures and DNA-Cleaving Activities of $[Cemp]_2[MCl_4]$ (Cemp=*N*-Carbethoxymethyl-1,10-Phenanthrolinium, M=Cu(Ⅱ), Zn(Ⅱ), Co(Ⅱ), Ni(Ⅱ) and Mn(Ⅱ)). *Chem. Pharm. Bull.*, **2013**, **61**(7):714-721

[26]Pang J Y, Qin Y, Chen W H, Luo G A, Jiang Z H. Synthesis and DNA-Binding Affinities of Monomodified Berberines. *Bioorg. Med. Chem.*, **2005**,**13**(20):5835-5840

[27]Molecular Operating Environment (MOE). *Chemical Computing Group Inc.*, **2014**.

[28]Pettersen E F, Goddard T D, Huang C C, Couch G S, Greenblatt D M, Meng E C, Ferrin T E. UCSF Chimera-A Visualization System for Exploratory Research and Analysis. *J. Comput. Chem.*, **2004**,**25**(13): 1605-1612

[29]Liao G L, Chen X, Wu J H, Qian C, Wang Y, Ji L N, Chao H. Ruthenium(Ⅱ) Polypyridyl Complexes as Dual Inhibitors of Telomerase and Topoisomerase. *Dalton Trans.*, **2015**,**44**(34):15145-15156

[30]Schrödinger L L C. *The PyMOL Molecular Graphics System, Version* 1.8, **2015**.

[31]高春艳, 乔佩佩, 杨皇泽, 张鹏飞, 雷云博, 张永坡, 王敏, 岳爱琴, 赵晋忠, 杜维俊. 吡啶类单核钴(Ⅱ)配合物的合成、结构、与DNA的相互作用及细胞毒性. 无机化学学报, **2020**,**36**(9):1783-1790
GAO C Y, QIAO P P, YANG H Z. ZHANG P F, LEI Y B, ZHANG Y P, WANG M, YUE A Q, ZHAO J Z, DU W J. Synthesis, Structure, DNA Interaction and Cytotoxicity of Pyridine-Based Mononuclear Cobalt(Ⅱ) Complex. *Chinese J. Inorg. Chem.*, **2020**,**36**(9):1783-1790

[32]Schroeder G K, Lad C, Wyman P, Williams N H, Wolfenden R. The Time Required for Water Attack at the Phosphorus Atom of Simple Phosphodiesters and of DNA. *Proc. Natl. Acad. Sci. U. S. A.*, **2006**, **103**(11):4052-4055

[33]Xu W, Craft J A, Fontenot P R, Barens M, Knierim K D, Albering J H, Mautner F A, Massoud S S. Effect of the Central Metal Ion on the Cleavage of DNA by $[M(TPA)Cl]ClO_4$ Complexes (M=$Co^{Ⅱ}$, $Cu^{Ⅱ}$ and $Zn^{Ⅱ}$, TPA=Tris(2-pyridylmethyl)amine): An Efficient Artificial Nuclease for DNA Cleavage. *Inorg. Chim. Acta*, **2011**,**373**(1):159-166

[34]Roy M, Santhanagopal R, Chakravarty A R. DNA Binding and Oxidative DNA Cleavage Activity of (μ-oxo)Diiron(Ⅲ) Complexes in Visible Light. *Dalton Trans.*, **2009**,**12**(6):1024-1033

[35]Boerner L J K, Zaleski J M. Metal Complex-DNA Interactions: from Transcription Inhibition to Photoactivated Cleavage. *Curr. Opin. Chem. Biol.*, **2005**,**9**(2):135-144

[36]Arjmand F, Sayeed F, Muddassir M. Synthesis of New Chiral Heterocyclic Schiff Base Modulated Cu(Ⅱ)/Zn(Ⅱ) Complexes: Their Comparative Binding Studies with CT-DNA, Mononucleotides and Cleavage Activity. *J. Photochem. Photobiol. B*, **2011**,**103**(2):166-179

[37]Gómez-Saiz P, Gil-García R, Maestro M A, Pizarro J L, Arriortua M I, Lezama L, Rojo T, González-Álvareze M, Borráse J, García-Tojal J. Structure, Magnetic Properties and Nuclease Activity of Pyridine-2-carbaldehyde Thiosemicarbazonecopper (Ⅱ) Complexes. *J. Inorg. Biochem.*, **2008**,**102**(10):1910-1920

[38]Chen G J, Qiao X, Qiao P Q, Xu G J, Xu J Y, Tian J L, Wen G, Liu X, Yan S P. Synthesis, DNA Binding, Photo-Induced DNA Cleavage, Cytotoxicity and Apoptosis Studies of Copper(Ⅱ) Complexes. *J. Inorg. Biochem.*, **2011**,**105**(2):119-126

[39]Huang Y, Lu Q S, Zhang J, Zhang Z W, Zhang Y, Chen S Y, Li K, Tan X Y, Lin H H, Yu X Q. DNA Cleavage by Novel Copper(Ⅱ) Complex and the Role of β-Cyclodextrin in Promoting Cleavage. *Bioorg. Med. Chem.*, **2008**,**16**(3):1103-1110

[40]Qin D D, Yang Z Y, Wang B D. Spectra and DNA-Binding Affinities of Copper(Ⅱ), Nickel(Ⅱ) Complexes with a Novel Glycine Schiff Base Derived from Chromone. *Spectroc. Acta Pt. A-Molec. Biomolec. Spectr.*, **2007**,**68**(3):912-917

[41]Gao E J, Feng Y H, Su J Q, Meng B, Jia B, Qi Z Z, Peng T T, Zhu M C. Synthesis, Characterization, DNA Binding, Apoptosis and Molecular Docking of Three Mn(Ⅱ), Zn(Ⅱ) and Cu(Ⅱ) Complexes with Terpyridine-Based Carboxylic Acid. *Appl. Organomet. Chem.*, **2017**,**32**(3): e4164

[42]Haribabu J, Jeyalakshmi K, Arun Y, Bhuvanesh N S P, Perumal P T, Karvembu R. Synthesis, DNA/Protein Binding, Molecular Docking, DNA Cleavage and *In Vitro* Anticancer Activity of Nickel(Ⅱ) Bis (thiosemicarbazone) Complexes. *RSC Adv.*, **2015**,**5**(57):46031-46049

[43]Basheer S M, Rasin P, Kumar S L A, Kumar M S, Sreekanth A. Investigation on DNA/Protein Interaction of Thiosemicarbazone Based Octahedral Nickel(Ⅱ) and Iron(Ⅲ) Complexes. *J. Mol. Struct.*, **2022**,**1260**:132913